Computational study of oxygen stability in vicinal m(10-10)-GaN growth by MOVPE

Shintaku, Fumiya
Department of Aeronautics and Astronautics, Kyushu University

Yosho, Daichi
Department of Aeronautics and Astronautics, Kyushu University

Kangawa, Yoshihiro
Department of Aeronautics and Astronautics, Kyushu University

Iwata, Jun-Ichi
AdvanceSoft Corporation

他

出版情報：Applied Physics Express. 13 (5), pp.055507-1-055507-4, 2020-05. IOP Publishing
バージョン：

Computational study of oxygen stability in vicinal m(10−10)-GaN growth by MOVPE

Fumiya Shintaku[1], Daichi Yosho[1], Yoshihiro Kangawa[1, 2, 3] *, Jun-Ichi Iwata[4], Atsushi Oshiyama[3], Kenji Shiraishi[3], Atsushi Tanaka[3], and Hiroshi Amano[3]

[1]*Department of Aeronautics and Astronautics, Kyushu University, Fukuoka 819-0395, Japan*

[2]*Research Institute for Applied Mechanics (RIAM), Kyushu University, Fukuoka 816-8580, Japan*

[3]*Institute of Materials and Systems for Sustainability (IMaSS), Nagoya University, Nagoya 464-8601, Japan*

[4]*AdvanceSoft Corporation, Tokyo 101-0062, Japan*

* E-mail: kangawa@riam.kyushu-u.ac.jp

Abstract:

Using density functional calculations, we clarify the oxygen incorporation mechanism in vicinal m-GaN growth by metal organic vapor-phase epitaxy. We first identify reconstructed structures of 5° off m-GaN toward the ±c directions. Next, we explore preferable sites for oxygen substitution near step edges. We find that oxygen prefers the lower nitrogen site of the step edge on the +c 5° off m-GaN substrate compared with that on the –c 5° off m-GaN substrate. This tendency agrees with recent experimental findings that the oxygen concentration in −c 5° off m-GaN epilayers is lower than that in +c 5° off m-GaN epilayers.

Gallium nitride (GaN)-based devices for optics and high-power electronics are widely considered attractive due to their excellent physical properties, such as a direct wide band gap, high electron mobility and high thermal conductivity.[1-5] For optical devices, unintentionally doped impurities, such as oxygen, into GaN or InGaN active layers induce energy states in the band gap. Such doping causes unintended luminescence, such as "yellow luminescence".[6] For power devices, the breakdown voltage is affected by the carrier concentration. It is known that unintentionally doped oxygen into GaN layers substitutes for nitrogen sites and behaves as a shallow donor. A high breakdown voltage over 1 kV requires an impurity concentration less than 10^{16} cm^{-3} in the active layers.[7] That is, for applications, it is essential to both clarify the impurity incorporation mechanism and control its concentration during growth. There have been considerable research reports[8-17] on the reduction of impurities in the case of polar plane growth, such as ±c(000±1)-plane growth, because the resulting materials have many practical uses, such as light emitting diodes (LEDs) or high-electron-mobility transistors (HEMTs). On the other hand, there are few reports[18] about impurity incorporation in the case of nonpolar plane growth, such as m(10−10)-plane growth, although layers grown without a polarization field along the growth direction have the advantage of improving the material's optical and electronic properties. In 2018, Tanaka et al.[19] reported that the oxygen concentration in GaN films grown on –c 5° off m-GaN by metal-organic vapor-phase epitaxy (MOVPE) was one order of magnitude below that on +c 5° off m-GaN. It is crucial to understand the reduction mechanism of oxygen concentration in vicinal m-GaN layers from both scientific and technological viewpoints. In the present study, we investigated the oxygen incorporation mechanism in vicinal m-GaN layers by a theoretical approach.

Revealing step edge structures, i.e., starting model, is necessary to investigate the oxygen incorporation mechanism during step-flow growth. Hence, we determined the stable reconstructed structures of step edges on ±c 5° off m-GaN during MOVPE under H_2 carrier gas conditions. To analyze the relationship between the reconstructed structures and growth conditions such as temperature and partial pressure, we used the theoretical approach proposed by Kangawa et al.[20] in 2001. The surface with the lowest surface formation energy will appear at equilibrium. The surface formation energy is written as

$$E_{\mathrm{f}} = E_{\mathrm{surface}}^{\mathrm{recon}} - E_{\mathrm{surface}}^{\mathrm{ideal}} - n_{\mathrm{Ga}}^{\mathrm{ad}}\left(E_{\mathrm{Ga}}^{\mathrm{gas}} - \mu_{\mathrm{Ga}}^{\mathrm{gas}}\right) - \frac{1}{2}n_{\mathrm{N}}^{\mathrm{ad}}\left(E_{\mathrm{N2}}^{\mathrm{gas}} - \mu_{\mathrm{N2}}^{\mathrm{gas}}\right) - \frac{1}{2}n_{\mathrm{H}}^{\mathrm{ad}}\left(E_{\mathrm{H2}}^{\mathrm{gas}} - \mu_{\mathrm{H2}}^{\mathrm{gas}}\right), \quad (1)$$

where $E_{\mathrm{surface}}^{\mathrm{ideal}}$ and $E_{\mathrm{surface}}^{\mathrm{recon}}$ are the total energies at absolute zero of the ideal and reconstructed surface systems, respectively. $E_{\mathrm{Ga}}^{\mathrm{gas}}$, $E_{\mathrm{N2}}^{\mathrm{gas}}$, and $E_{\mathrm{H2}}^{\mathrm{gas}}$ are the total energies at absolute zero of Ga, N_2, and H_2 molecules, respectively. $\mu_{\mathrm{Ga}}^{\mathrm{gas}}$, $\mu_{\mathrm{N2}}^{\mathrm{gas}}$, and $\mu_{\mathrm{H2}}^{\mathrm{gas}}$ are the chemical potentials at the growth temperatures and partial pressures of Ga, N_2, and H_2 molecules, respectively. $n_{\mathrm{Ga}}^{\mathrm{ad}}$, $n_{\mathrm{N}}^{\mathrm{ad}}$, and $n_{\mathrm{H}}^{\mathrm{ad}}$ are the numbers of Ga, N, and H adatoms on the reconstructed surface, respectively. In Eq. (1), the temperature dependence of the energy and the entropy effects of the surface system are neglected to consider only the total energy at absolute zero, $E_{\mathrm{surface}}^{\mathrm{ideal}}$ and $E_{\mathrm{surface}}^{\mathrm{recon}}$. The chemical potential of a gas molecule is provided as a function of the temperature T and partial pressure p:

$$\mu = -k_B T \ln\left(\frac{g k_B T}{p} \times \zeta_{\mathrm{trans}}\zeta_{\mathrm{rot}}\zeta_{\mathrm{vibr}}\right), \quad (2)$$

$$\zeta_{\mathrm{trans}} = \left(\frac{2\pi m k_B T}{h^2}\right)^{\frac{3}{2}}, \quad (3)$$

$$\zeta_{\mathrm{rot}} = \frac{1}{\pi\sigma}\left[\frac{8\pi^3 (I_A I_B \cdots)^{\frac{1}{n}} k_B T}{h^2}\right]^{\frac{n}{2}}, \quad (4)$$

$$\zeta_{\mathrm{vibr}} = \prod_i^{3N-3-n}\left[1 - \exp\left(-\frac{h\nu_i}{k_B T}\right)\right]^{-1}, \quad (5)$$

where ζ_{trans}, ζ_{rot}, and ζ_{vibr} are the partition functions for translational, rotational, and vibrational motions,

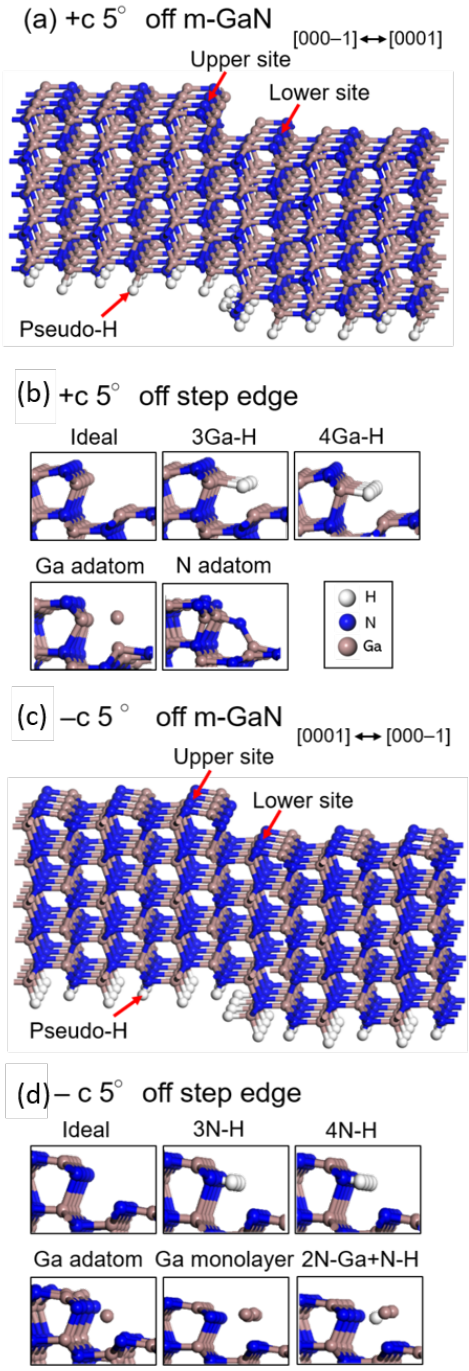

Fig. 1. (a), (c) Schematics of +c 5° off and –c 5° off m-GaN, respectively. (b), (d) Candidate reconstructed structures of the step edge considered in this study.3Ga-H, 4Ga-H, Ga adatom, and N adatom in (b) mean three of four Ga at the step edge are terminated by H, four Ga are terminated by H, one Ga is adsorbed at the step edge, and one N is adsorbed at the step edge, respectively. 3N-H, 4N-H, Ga adatom, Ga monolayer, and 2N-Ga+N-H in (d) mean three of four N at the step edge are terminated by H, four N are terminated by H, one Ga is adsorbed at the step edge, four Ga are adsorbed at the step edge, two Ga and one H are adsorbed at the step edge, respectively.

respectively. k_B is Boltzmann's constant, h is Planck's constant, T is temperature, p is pressure, g is the degree of degeneracy of the electron energy level, m is the mass of one particle, n is the degree of freedom for rotation, σ is the symmetric factor, I_I is the moment of inertia, i is the degree of freedom for vibration, N is the number of atoms in the particle, and ν is the frequency. Using Eqs. (1)-(5), the surface formation energy is provided as a function of temperature T and partial pressure p. The total energies at absolute zero are given by density functional calculations.

The total energies of the step edges on ±c 5° off m-GaN were calculated by using real-space density functional theory (RSDFT) as implemented in the RSDFT package.[21,22,23] The exchange and correlation energies were treated by the Perdew-Burke-Ernzerhof (PBE)[24] exchange correlation functional using the norm-conserving pseudopotentials.[25] Ga3d electrons were treated as core electrons. The mesh spacing was fine enough to correspond to the cutoff energy of 108 Ry on the conventional plane-wave basis. For surface calculation, we used a periodic slab composed of 532 atoms (+ adatoms). Fig. 1(a) and 1(c) show schematics of the +c 5° off and –c 5° off m-GaN models, respectively. The slab model comprised a vacuum layer of more than 20 Å, five GaN bilayers in height, and four GaN bilayers in depth. The width of terrace in the slab model was determined to reproduce 5° off angles toward [0001] and [000-1]. Ga and N dangling bonds at the bottom surface of the slab model were terminated by pseudo-hydrogens of charge 1.25e and 0.75e, respectively, to mimic a semi-infinite GaN substrate.[26] The epilayers and adatoms were allowed to relax until the force acting on each atom was less than 5×10^{-4} Hartree/a.u. (atomic units), while the bottom layers and pseudo-hydrogens were kept fixed to mimic bulk-like behavior.

Fig. 1(b) and 1(d) show the candidate reconstructed structures of the ±c 5° off step edges considered in this study. These candidate structures were constructed based on our previous knowledge.[27, 28] The number of candidate structures seems enough since the possible configuration of adatoms at one dimensional step edge instead of two dimensional surface is very limited. It has been reported that the stable terrace structure is the unreconstructed ideal surface without adsorbates[29] under the same conditions as those used experimentally[19]: H_2 carrier gas, total pressure of 1 atm, T = 1100 °C, and V/III = 1019. The stable reconstructed structure of ±c 5° off step edges was then analyzed by adopting such an ideal terrace. The surface formation energy was determined by Eq. (1). Under the same growth conditions as those used experimentally[19], the surface formation energies of each step edge structure as a function of temperature were calculated and are shown in Fig. 2(a) and 2(c). We have found that particular step edge for each vicinal direction shows the lowest formation energy in a certain range of temperature. That is, the ideal and 3N-H structures appear for the +c 5° off and –c 5° off step edges, respectively, under the following experimental growth conditions: T = 1100 °C, V/III = 1019[19]. Here, the ideal step edge means a bare step edge without any adsorbed atom, and 3N-H means a three-hydrogen-terminated step edge. The ideal step edge model does not satisfy the electron counting (EC) rule[30, 31], though 3N-H structure satisfy the EC rule: when nitrogen dangling bonds that remain on the surface are filled with two electrons while gallium dangling bonds are empty, the system is energetically favorable. In the case of +c 5° off, one can see 3Ga-H structure which satisfy the EC rule appears at low temperatures (Fig. 2(a)). The chemical potential of H_2 molecule decreases with increase of temperature (see eq. (2)). Hence, H-terminated step edge which satisfy the EC rule appears at low temperatures, but ideal step edge which does not satisfy the EC rule appears at high temperatures since H_2 molecule becomes stable in the vapor phase than on the surface. In the case of +c 5° off, the critical temperature between the two

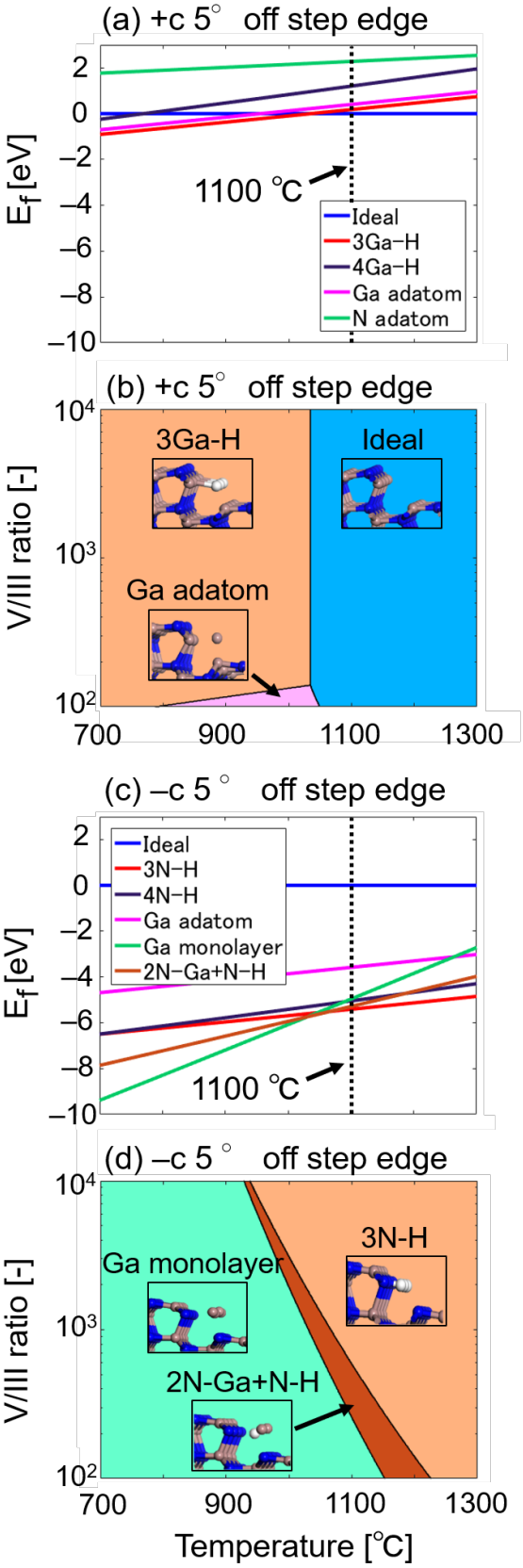

Fig. 2. (a), (c) Surface formation energy of the +c 5° off and –c 5° off step edges as a function of temperature, respectively, under the same conditions as those used experimentally: carrier gas ratio of p_{H2}:p_{N2} = 0.6 atm: 0.2 atm, V/III ratio of 1019. (b), (d) Surface phase diagram of the +c 5° off and –c 5° off step edges, respectively.

Table I. The calculated formation energies ΔE_{O_N} in eV.

	+c 5° off	−c 5° off
Upper site of step edge	−0.073	−0.031
Lower site of step edge	−0.91	−0.13

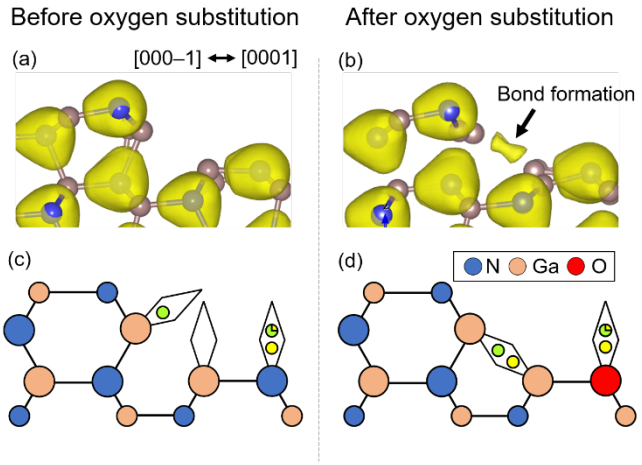

Fig. 3. (a), (b) Electron density around the step edge before and after oxygen substitution, respectively, in the case of +c 5° off. (c), (d) Schematics of the electron counting model. Light green circles and three-quarter circles show electrons supplied from cation. Light yellow circles and a quarter circles show electrons supplied from anion. When an oxygen atom substitute for nitrogen (d), one excess electron is supplied from oxygen to gallium to make Ga-Ga bond. In this system, EC rule is satisfied.

surface phases appears around 1030°C (Fig. 2(a)), it will appear at more high temperature in the case of –c 5° off (Fig. 2(c)). This is because N-H bond is stronger than Ga-H bond. Fig. 2(b) and 2(d) show surface phase diagrams of ±c 5° off step edges as a function of temperature and V/III ratio. In the case of growth conditions other than those used experimentally[19], other structures appear.

Next, the formation energies of oxygen substituting nitrogen, O_N, at the upper and lower sites of thus obtained step edges were calculated by using the predicted surface model as the starting model. In the present research, we considered only O_N because the formation of the point defect is most often predicted in first principles calculations.[32] The O_N formation energy ΔE_{O_N} at the upper and lower sites of the step edge is expressed as

$$\Delta E_{O_N} = E_{\text{substitute}} - E_{\text{reference}}, \qquad (6)$$

where $E_{\text{substitute}}$ is the total energy of a system whose upper or lower step edge is substituted by an oxygen atom. $E_{\text{reference}}$ is the total energy of a system whose nitrogen site on the terrace is substituted by an oxygen atom. The calculated formation energies ΔE_{O_N} are summarized in Table I. In the case of –c 5° off, there are three different cases of substitution sites due to their positional relationship with the hydrogen-terminated step edge. The calculated ΔE_{O_N} values of the three cases are different. Thus, –c 5° off yields the lowest ΔE_{O_N} among the calculated values. The calculation results suggest that oxygen at the lower site of the +c 5° off step edge is the most stable as shown in Table I. The results imply that the oxygen incorporation ratio at the step edge on +c 5° off m-GaN would be higher than that on –c 5° off m-GaN. This tendency agrees with the experimental results.

Hereafter, we discuss the reason why the ΔE_{O_N} values are different between the upper and lower sites of the +c 5° off step edge from the viewpoint of the EC model. Fig. 3(a) and 3(b) show the electron density around the step edge on +c 5° off m-GaN. The electron density was visualized by VESTA[33, 34]. Fig. 3(c) and 3(d) show schematics of the EC model around the step edges before and after oxygen substitution, respectively, in the case of the +c 5° off substrate. In the case of GaN, nitrogen

donates 5/4 electrons and gallium donates 3/4 electrons for a single covalent bond. On the ideal surface of the m-plane, nitrogen dangling bonds receive electrons from gallium and have two electrons. On the other hand, gallium dangling bonds, which have lost electrons, are empty. That is, the ideal surface of the m-plane satisfies the EC rule. In the case of +c 5° off m-GaN, the dangling bonds of the ideal step edge terminated by four gallium atoms per supercell have three electrons (= 4 x (3/4) electrons). This condition does not satisfy the EC rule (Fig. 3(a) and (c)). Upon O_N formation at the lower step edge, one excess electron is supplied from an oxygen to the gallium dangling bond near the step edge. That is, four electrons accumulate near the step edge. Consequently, two Ga-Ga bonds are formed between the gallium terminating the step edge and the gallium at the lower step edge (Fig. 3(b) and 3(d)). Therefore, no electrons remain in the gallium dangling bonds on the step in this model. As a result, the EC rule is satisfied, and the system of the step edge becomes energetically stable. On the other hand, the O_N at the upper step edge bonds to three gallium atoms each of which has a single dangling bond, while the O_N at the lower step edge bonds to one gallium atom which has a single dangling bond and two gallium atoms each of which has no dangling bond. Therefore, the former system, i.e., O_N at the upper step edge, does not satisfy the EC rule, since one excess electron supplied from an oxygen seems distribute to the three gallium dangling bonds instead of the use for formation of Ga-Ga bonds at the step edge. The above discussion reveals the reason why O_N prefers a lower step edge. In the case of –c 5° off m-GaN, the starting model, i.e., the 3N-H step edge, already satisfies the EC rule. Therefore, bond rearrangement with superior energy gain will not occur after oxygen substitution. Thus, a preferable site for oxygen substitution did not appear in this system. This tendency was also confirmed for other systems, i.e., O_N at the terrace and 2nd layer (not shown here).

In summary, we have revealed the stable reconstructed structures on vicinal m-GaN during MOVPE. The formation energies of the system in which oxygen substitutes for nitrogen at the upper and lower sites of the step edge were calculated by using the predicted surface model as the starting model. The calculated results explain the experimental oxygen incorporation tendency. This theoretical approach is helpful to understand the oxygen incorporation mechanism and physics of such phenomena. This knowledge is also useful for optimizing growth conditions to obtain m-GaN with low oxygen concentrations by MOVPE.

Acknowledgments

This work was partially supported by the MEXT "Program for Research and Development of Next-Generation Semiconductors to Realize an Energy-Saving Society (Grant Number JPJ005357)", MEXT "Social and Scientific Priority Issue: Creation of New Functional Devices and High-Performance Materials to Support Next-Generation Industries by post-K Computer", JSPS KAKENHI (Grant Number JP16H06418), JST SICORP (Grant Number 16813791B), and the European Union's Horizon 2020 Research and Innovation Program (Grant Number 720527: InRel-NPower project). The computations were carried out using the computer resources offered under the category of general projects by the Research Institute for Information Technology, Kyushu University.

References

1) H. Amano, Y. Baines, E. Beam, M. Borga, T. Bouchet, P. R. Chalker, M. Charles, K. J. Chen, N. Chowdhury, R. Chu, C. De Santi, M. M. De Souza, S. Decoutere, L. Di Cioccio, B. Eckardt, T. Egawa, P. Fay, J. J. Freedsman, L. Guido, O. Häberlen, G. Haynes, T. Heckel, D. Hemakumara, P. Houston, J. Hu, M. Hua, Q. Huang, A. Huang, S. Jiang, H. Kawai, D. Kinzer, M. Kuball, A. Kumar, K. B. Lee, X. Li, D. Marcon, M. März, R. McCarthy, G. Meneghesso, M. Meneghini, E. Morvan, A. Nakajima, E. M. S. Narayanan, S. Oliver, T. Palacios, D. Piedra, M. Plissonnier, R. Reddy, M. Sun, I. Thayne, A. Torres, N. Trivellin, V. Unni, M. J. Uren, M. Van Hove, D. J. Wallis, J. Wang, J. Xie, S. Yagi, S. Yang, C. Youtsey, R. Yu, E. Zanoni, S. Zeltner, and Y. Zhang, J. Phys. D: Appl. Phys. **51**, 163001 (2018).
2) Y. Zhang, A. Dadgar, and T. Palacios, J. Phys. D: Appl. Phys. **51**, 273001 (2018).
3) A. Tanaka, W. Choi, R. Chen, and S. A. Dayeh, Adv. Mater. **29**, 1702557 (2017).
4) K. Shojiki, T. Tanikawa, J. H. Choi, S. Kuboya, T. Hanada, R. Katayama, and T. Mtsuoka, Appl. Phys. Express 8, 061005 (2015).
5) M. Kushimoto, T. Tanikawa, Y. Honda, and H. Amano, Appl. Phys. Express 8, 022702 (2015).
6) K. Kojima, F. Horikiri, Y. Narita, T. Yoshida, H. Fujikura, and S. F. Chichibu, Appl. Phys. Express, **13**, 012004 (2020).
7) T. Kachi, Jpn. J. Appl. Phys. **53**, 100210 (2014).
8) N. A. Fichtenbaum, T. E. Mates, S. Keller, S. P. DenBaars, and U. K. Mishra, J. Cryst. Growth **310**, 1124 (2008).
9) D. D. Koleske, A. E. Wickenden, R. L. Henry, and M. E. Twigg, J. Cryst. Growth **242**, 55 (2002).
10) J.-L. Zhang, J.-L. Liu, Y. Pu, W.-Q. Fang, M. Zhang, and F.-Y. Jiang, Chin. Phys. Lett. **31**, 037102 (2014).
11) Q. Mao, J. Liu, X. Wu, J. Zhang, C. Xiong, C. Mo, M. Zhang, and F. Jiang, J. Semicond. **36**, 093003 (2015).
12) F. Kaess, S. Mita, J. Xie, P. Reddy, A. Klump, L. H. Hernandez-Balderrama, S. Washiyama, A. Franke, R. Kirste, A. Hoffmann, R. Collazo, and Z. Sitar, J. Appl. Phys. **120**, 105701 (2016).
13) W. V. Lundin, A. V. Sakharov, E. E. Zavarin, D. Y. Kazantsev, B. Y. Ber, M. A. Yagovkina, P. N. Brunkov, and A. F. Tsatsulnikov, J. Cryst. Growth **449**, 108 (2016).
14) G. Piao, K. Ikenaga, Y. Yano, H. Tokunaga, A. Mishima, Y. Ban, T. Tabuchi, and K. Matsumoto, J. Cryst. Growth **456**, 137 (2016).
15) T. Tanikawa, S. Kuboya, and T. Matsuoka, Phys. Status Solidi B **254**, 1600751 (2017).
16) Y. Inatomi, Y. Kangawa, A. Pimpinelli, and T. L. Einstein, Phys. Rev. Mater. **3**, 013401 (2019)
17) T.-T. Yuan, P.-Y. Kuei, L.-Z. Hsieh, T.-C. Li, and W.-J. Lin, J. Cryst. Growth **312**, 2239 (2010).
18) A. Tanaka, O. 1. Barry, K. Nagamatsu, J. Matsushita, M. Deki, Y. Ando, M. Kushimoto, S. Nitta, Y. Honda, and H. Amano, Phys. Status Solidi (a) **214**, 1600829 (2017).
19) A. Tanaka, Y. Ando, K. Nagamatsu, M. Deki, H. Cheong, B. Ousmane, M. Keshimoto, S. Nitta, Y. Honda, and H. Amano, Phys. Status Solidi (a) **215**, 1700645 (2018).
20) Y. Kangawa, T. Ito, A. Taguchi, K. Shiraishi, and T. Ohachi, Surf. Sci. 493, 178 (2001).
21) J.-I. Iwata, D. Takahashi, A. Oshiyama, T. Boku, K. Shiraishi, S. Okada, and K. Yabana, J. Comput. Phys. **229**, 2339 (2010).
22) Y. Hasegawa, J.-I. Iwata, M. Tsuji, D. Takahashi, A. Oshiyama, K. Minami, T. Boku, H. Inoue, Y. Kitazawa, I. Miyoshi, M. Yokokawa, Int. J. High Perform. Comput. Appl. **28**, 335 (2014).

23) J.-I. Iwata, RSDFT public page, https://github.com/j-iwata/RSDFT, (accessed 2020.03.01)
24) J. P. Perdew, K. Burke, and M. Ernzerhof, Phys. Rev. Lett. **77**, 3865 (1996).
25) N. Troullier and J. L. Martins, Phys. Rev. B **43**, 1993 (1991).
26) K. Shiraishi, J. Phys. Soc. Jpn. **59**, 3455 (1990).
27) Y. Kangawa, T. Akiyama T. Ito, K. Shiraishi, T. Nakayama, Materials **6**, 3309 (2013).
28) T. Matsuoka, Y. Kangawa (eds.), Epitaxial Growth of III-Nitride Compounds: Computational Approach, Springer Series in Materials Science, **269** (2018).
29) A. Kusaba, Y. Kangawa (private communications).
30) M.D. Pashley, K.W. Haberern, W. Friday, J.M. Woodall, and P.D. Kirchner: Phys. Rev. Lett. **60**, 2176 (1988).
31) M. D. Pashley, Phys. Rev. B **40**, 10481 (1989).
32) A. F. Wright, J. Appl. Phys. **98**, 103531 (2005)
33) K. Momma and F. Izumi, J. Appl. Crystallogr. **41**, 653 (2008).
34) K. Momma and F. Izumi, J. Appl. Crystallogr. **44**, 1272 (2011).